CHAPTER 3

ANTENNA, METAMATERIAL AND FILTER DESIGN FUNDAMENTALS

3.1 INTRODUCTION

This Chapter provides the basics of MSAs, FAs, MTMs, IAs and LPF needed for the analytical designs. It provides many useful guidelines of how the design, simulation, testing of MTM properties and experiments can be carried out. The contents of this Chapter have been used for the designs of various proposed antennas throughout the thesis.

3.2 BASICS OF THE MSA

MSAs can be designed using the planar technology (Kai Fong Lee, 2011**)**. In general, in MSA based antennas, the radiation from microstrip occurs due to fringing fields between the patch and the ground. Moreover, the radiation efficiency and signal speed depend on the dielectric permittivity ε_r of the substrate material. Thick dielectric, low ε_r and low loss tangent are preferred for improved efficiency and broadband purposes.

3.2.1 Design Fundamental

The Figure 3.1 shows the general outlook of the MSA with all dimensions in millimeters. The design parameters (Gupta and Abdelaziz Benalla 1988, Samuel Liao 2006) and geometries of antennas include resonant frequency f_r, characteristic impedance Z_0, substrate permittivity ε_r,

substrate thickness h, antenna width W, width to height ratio W/h, effective permittivity ε_{eff}, antenna Length L; for CPW feed the center strip length L_s and slot width w_s; for microstrip feed, the length of feed may be of the order of quarter wavelength or its multiples and the ground plane width W_g and length L_g; but practically they can be of the same dimensions as that of substrate under the antenna.

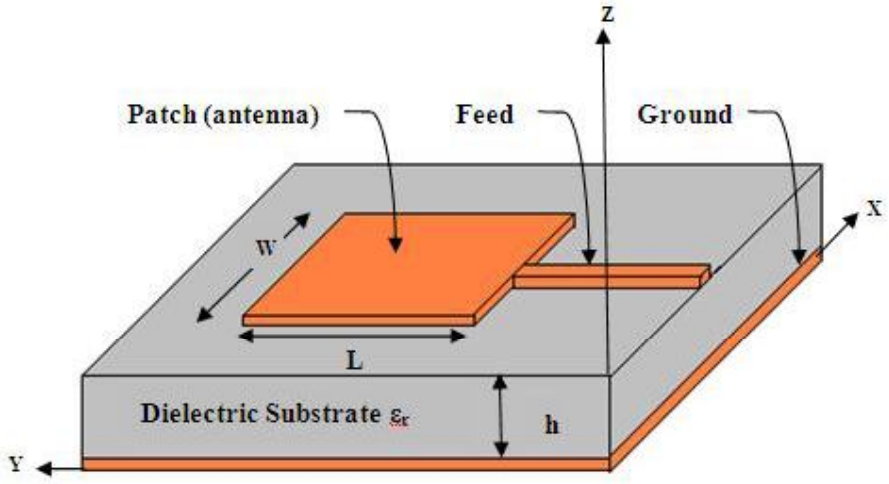

Figure 3.1 A General Microstrip Fed MSA Structure

The following set of Equations from (3.1) to (3.10) play vital role in determining all the dimensions relating to antenna design. The width (W) to thickness (h) ratio is given by

$$\frac{W}{h} = \frac{8\,e^{A}}{e^{2A}-2} \tag{3.1}$$

where $A = \frac{Z_o}{6}\left[\frac{\varepsilon_r+1}{2}\right]^{1/2} + \frac{\varepsilon_r-1}{\varepsilon_r+1}\left[0.23 + \frac{0.11}{\varepsilon_r}\right]$ (3.2)

The characteristic impedance Z_0 is normally considered to be 50 ohms for matching conditions. Depending on whether $W/h > 1$ or $W/h > 1$, one can choose the appropriate formula for the determination of the effective

medium property, since the MSA involves quasi-TEM mode of propagation because of the existence of EM waves in substrate as well as air media which is shown in Figure 3.2. Hence

a. If $W/h < 1$, then Equations (3.3) and (3.4) may be chosen

$$\varepsilon_{eff} = \left[\frac{\varepsilon_r+1}{2}\right] + \left[\frac{\varepsilon_r-1}{2}\right]\left[\left(1+\frac{12h}{W}\right)^{-\frac{1}{2}} + 0.04\left(1-\frac{W}{h}\right)\right]^2 \quad (3.3)$$

$$Z_o = \frac{60}{\sqrt{\varepsilon_{eff}}}\ln\left[\left(\frac{8h}{W}\right) + 0.25\left(\frac{W}{h}\right)\right] \quad (3.4)$$

b. If $W/h \geq 1$, then Equations (3.5) and (3.6) may be used

$$\varepsilon_{eff} = \left[\frac{\varepsilon_r+1}{2}\right] + \left[\frac{\varepsilon_r-1}{2}\right]\left[1+\frac{12h}{W}\right]^{-1/2} \quad (3.5)$$

$$Z_o = \left[\frac{377}{\sqrt{\varepsilon_{eff}}}\right]\left[\frac{W}{h} + 1.393 + \left(\frac{2}{3}\right)\ln\left(\frac{W}{h} + 1.444\right)\right]^{-1} \quad (3.6)$$

Alternatively, the width of patch may also be calculated from Equation (3.7) as given below.

$$W = \left(\frac{c}{2f_r}\right)\left[\left(\varepsilon_{eff}\right)\right]^{-1/2} \quad (3.7)$$

where

c is speed of light (mm/s) = $3x10\text{^}100$ mm/sec (also velocity of microwave)

f_r is the resonant frequency (GHz)

W is the width (mm) of the patch and

ε_{eff} is the effective permittivity of the medium

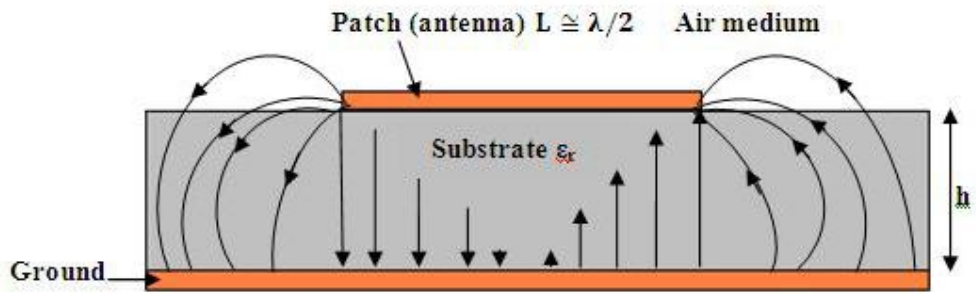

Figure 3.2 Fringing E Fields in MSA

If the MSA assumes rectangular shape then the length L of the patch may be determined from Equation (3.8), by taking the fringing effect as shown in Figure 3.2, into consideration. However, the length of the patch may also be considered to be half-a-wavelength or its multiples for better impedance matching. Therefore,

$$L = L_{eff} - 2\,\Delta L \tag{3.8}$$

where $L_{eff} = \left(\frac{c}{2f_r}\right)\left[\left(\varepsilon_{eff}\right)^{-0.5}\right]$ (3.9)

and $\Delta L = 0.412h\frac{\left[\left(\varepsilon_{eff}+0.3\right)\left(\frac{W}{h}+0.264\right)\right]}{\left[\left(\varepsilon_{eff}-0.258\right)\left(\frac{W}{h}+0.8\right)\right]}$ (3.10)

For the conventional ground plane, the length and width are determined as below.

$$L_g = 6h + L \tag{3.11}$$

$$W_g = 6h + W \tag{3.12}$$

3.2.2 Feeding methods

The feeding can be either contacting or non-contacting type. The type of feeding influences the input impedances and polarization

characteristics of antenna. Therefore, the effect of feeding mechanism is not simple any way. There are five popular methods used for feeding the MSAs as listed below:

- Microstrip line
- Coaxial probe
- Co-planar waveguide (CPW)
- Aperture coupled
- Proximity coupled

In all these feeding methods excepting CPW, the ground plane lies on the opposite side of the antenna layout insisting the need for double side printed substrate board. For modeling, simulation and fabrication, the microstrip feed remains to be very convenient. The CPW was invented by Cheng Wen (1969). The CPW offers some advantages of convenience and hence is used popularly in most antenna designs recently. It allows the usage thick substrates for obtaining broad bandwidths. It has no backside conducting part and therefore no thinning, etching, backside platting processes required. For CPW feed system the effective dielectric constant is very close to the average value of the relative dielectric constant of the substrate material and the free space dielectric constant. In CPW half of the electric filed lines are in dielectric medium and the rest half in the free space (or air) and therefore its dominant mode of propagation is quasi-TEM and hence it does not support pure TEM (Tatsuo Itoh 1989).

Some researchers (Shih-Ping Lin 1997, Thiruvalarchelvan and Raghavan 2009) used additional ground plane at the bottom of the substrate called conductor backed CPW. This mechanism offers advantage of heat

removal if this CPW is used along with active devices in monolithic microwave integrated circuits. However it suffers from two problems such as complexity in maintaining the quasi-TEM mode and to maintain the ground plane underneath at the same potential as that of CPW ground and hence extra care is to be taken to avoid such inconveniences.

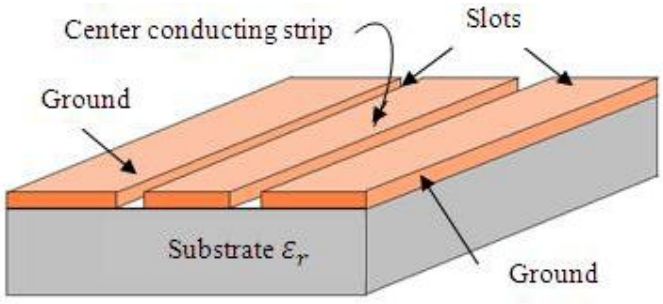

(a)

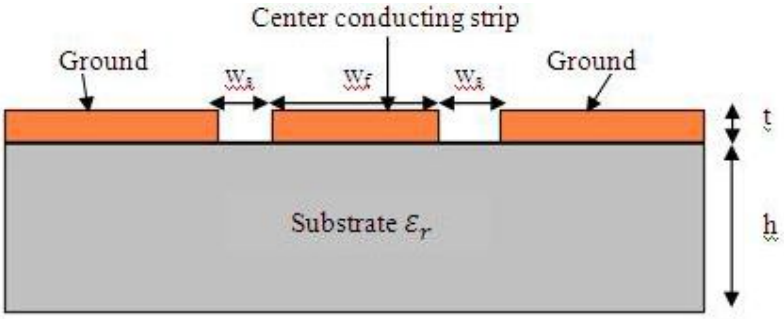

(b)

Figure 3.3 A CPW Structure (a) Perspective View (b) Front View

3.2.3 Feed Strip Dimensions of CPW

The CPW structure is shown in Figure 3.3. The design equations for CPW fed MSA are given in Equations (3.13) to (3.15). The characteristic impedance Z_0, the width w_f of the center conductor (feed strip) and slot width w_s in the CPW can be determined from the property ε_r of the dielectric substrate.

$$Z_0 = \frac{30\pi^2}{\sqrt{\varepsilon_{eff}}}\left[ln2\frac{(1+\sqrt{k})}{(1-\sqrt{k})}\right]^{-1} \quad (3.13)$$

when $t/w_s << 1$, $w_s/h << 1$ and $0.1 < k < 0.7$

$$k = \frac{w_f}{(w_f+2w_s)} \quad (3.14)$$

Since the filling factor of CPW is roughly around 50%, the effective permittivity is given by

$$\varepsilon_{eff} = \frac{\varepsilon_r+1}{2} \quad (3.15)$$

The VSWR and return loss may be calculated from the knowledge of the reflection parameter S_{11}. The lower the return loss the better is the matching at resonance. Hence a return loss of -9.5 dB itself corresponds to VSWR of 2. For a matched condition to exist the value of VSWR should be between 1 and 2. The VSWR is given by Equations (3.16) and (3.17).

$$VSWR = \frac{1+S_{11}}{1-S_{11}} \quad (3.16)$$

$$Return\ loss = -20\ log(S_{11}) \quad (3.17)$$

The corresponding MATLAB codings for MSA and microstrip feed of CPW are listed in Appendix 1.

3.3 BASICS OF THE FA

With a view to miniaturize the antenna size, if the dimensions of the MSA are made much smaller than its operating wavelength, then the radiation resistance, efficiency and bandwidth will get affected and reduced. However, the FAs can be much smaller in size than the operating wavelength without seriously affecting the other antenna parameters.

3.3.1 Various Fractal Structures

A variety of structures have already been proposed by many researchers. This includes Koch curves, Sierpinski gasket, Koch snowflake, fractal tree, Minkowski curve, Hilbert curve fractal antennas which are depicted in Figure 3.4.

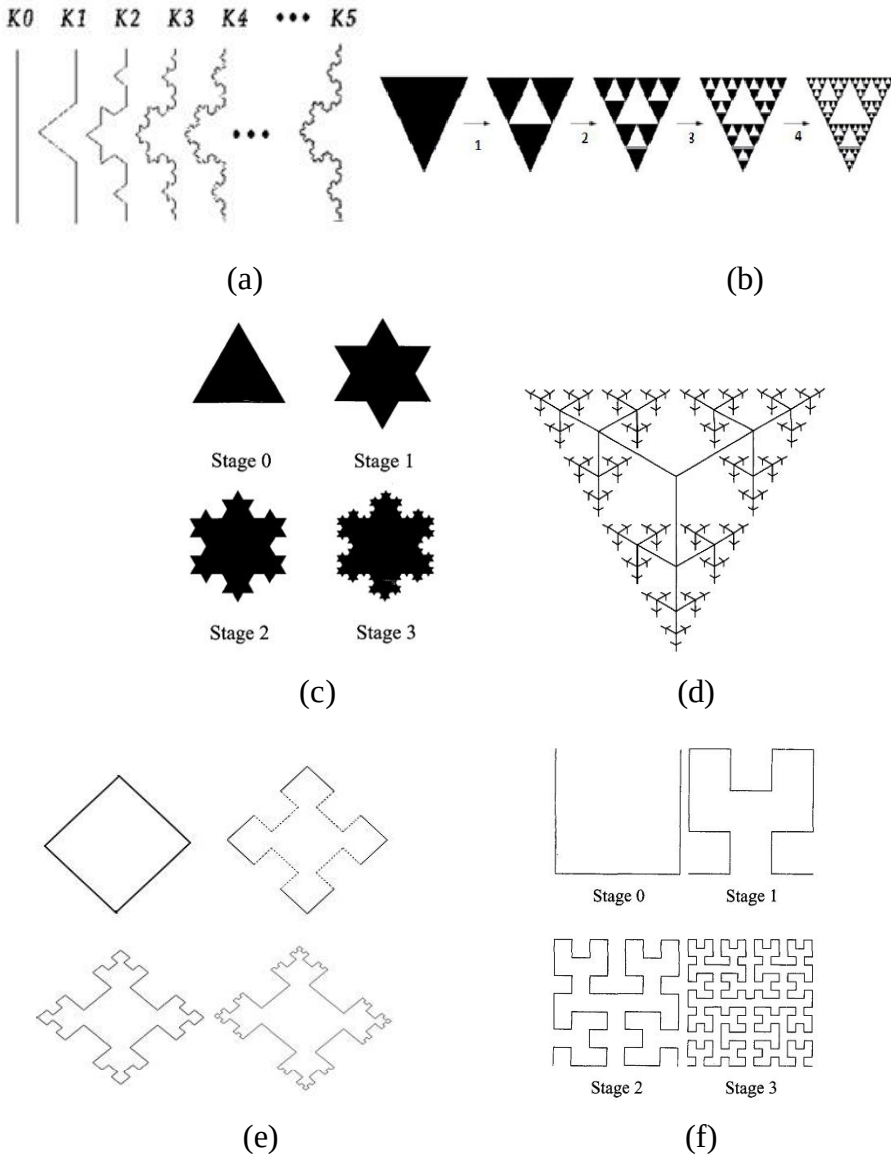

Figure 3.4 Different Fractal Curves (a) Koch Curves (b) Sierpinski Gasket (c) Koch Snowflake (d) Fractal Tree (e) Minkowski Curve (f) Hillbert Curve (Courtesy: Douglas Werner and Suman Ganguly 2003)

Though Peano introduced the first space filling curves in 1890 and Hilbert popularized the existence of the same in a modified form in 1891, there are different methods existing for generating space filling curves to improve bandwidth (Bially 1969) and different algorithms have been developed for the same (Goldschlager 1981, Greg Breinholt and Christoph Schierz 1998).

3.3.2 Hilbert Curve Resonance

This thesis covers the design of a modified HCFA from original Hilbert curve. Hence this section remains useful in the generation of the same from the fundamental monopole antenna. The stage 2 structure is considered for the design. For the Hilbert curve shown in Figure 3.5, the resonance (Dang-Oh Kim and Che-Young Kim 2012) can be obtained as given by Equations (3.18) to (3.21).

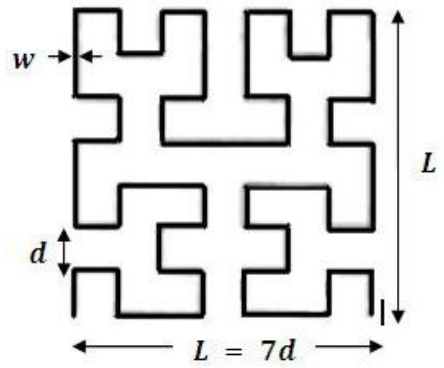

Figure 3.5 Second Iterated Hilbert Curve and Dimensions

$$S = (2^n - 1)d = (2^{\ n} + 1)L \tag{3.18}$$

$$d = \frac{L}{2^n - 1} \tag{3.19}$$

$$\frac{m\eta}{\pi\omega}\left[\frac{2d}{w}\right] tan\beta d + \frac{\mu_0}{\pi} S\left[log\frac{8S}{w} - 1\right] = \frac{\mu_0}{\pi}\frac{k\lambda}{4}\left[log\frac{8k\lambda}{4} - 1\right] \tag{3.20}$$

Therefore, $f_r = \frac{m\eta\left[\frac{2d}{w}\right]tan\beta d}{2\pi\mu_0\left\{\frac{k\lambda}{4}\left[log\frac{8k\lambda}{4}-1\right]-S\left[log\frac{8S}{w}-1\right]\right\}}$ (3.21)

where S = sum of all line segment

d = length of each line segment

n = the order of iteration

L = side dimension of Hilbert curve

$\lambda = 2\ L$ (the half-wavelength dipole antenna)

$m = 4^{\,n} - 1$

$\beta = \frac{2\pi}{\lambda}$

η = intrinsic impedance

w = width of the strip and

k = odd integer the harmonic component

The MATLAB coding for determining the resonance of Hilbert curve fractal antenna is provided in Appendix 2.

3.4 BASICS OF THE MTM

Materials with simultaneous negative permittivity and permeability referred to as left-handed materials. This concept was first theorized by Victor Veselago. He predicted that the EM planes in negative medium would propagate in a direction opposite to that of energy flow. After 32 years of its inception, the concept of MTMs was interestingly considered by investigators. Depending on the medium properties one can notice that there are different classes of MTMs.

3.4.1 Features of MTM

Some of the important features found in MTMs are reversal of Snell's law, unusual bending of EM waves in the backward direction, $\bar{E}, \bar{H}$ and Poynting Vector $\bar{P}$ following left handed rule, giving rise to the name left-handed metamaterial. This is explicitly shown in the following Maxwell's equations.

Conventional Substrate	Metamaterial
$\nabla X\bar{E} = -j\omega\bar{B}$(negative)	$\nabla X\bar{E} = j\omega\bar{B}$(positive)
$\nabla X\bar{H} = j\omega\bar{D} + \bar{J}$(positive)	$\nabla X\bar{H} = -[j\omega\bar{D} + \bar{J}]$(negative)

However, the scalar products of current density $\bar{J}$, electric flux density $\bar{D}$ and magnetic flux density $\bar{B}$ remain unchanged in both the cases. Left-handed materials support backward-waves and therefore have a negative refractive index. The wave propagation remains unchanged in the absence of sources and hence this unconventional result is noticed (David Smith and Norman Kroll 2000) from the Maxwell's curl equations and not from the wave equation. The backward wave propagation (phase propagation towards the source) occurs since the phase and group velocities move in opposite directions (Anthony Grbic and George Eleftheriades 2002). The phase velocity is the one at which the phase of any frequency component of the wave propagates whereas the group velocity is the one at which the envelope of the wave propagates. Hence the wavefronts move in the direction opposite to the flow of energy. The MTM structures are constructed as an array of conducting elements thus having suitable L and C characteristics. For microwave radiation to happen in MTMs, they should have dimensions much smaller than a wavelength.

3.4.2 Media and Components of MTM

At this stage it will be necessary to recall some important properties of various media. In anisotropic medium the property changes with respect to

the direction of propagation of wave. In the nonlinear medium the property changes non-linearly with change in electric field. When the property of medium is not constant and gradually varies with position, then it is termed as inhomogeneous medium. The medium in which the property remain same everywhere is recognized as homogeneous medium. For MTM to appear homogeneous, the structures would have to be electrically small and spaced electrically close. Christophe Caloz et al (2005) has presented the problems associated with homogenization of MTMs and elaborately discussed the methods of homogenization, the effect of change in unit cell and bandwidth enhancement. For designing the components of MTM structure (Ricardo Marques et al 2007) the microwave engineers use the dimensions given by Equation (3.22) to (3.25).

Size (unit cell) of the component : p (3.22)

Lumped components : $p < \lambda_g/4$ (3.23)

Quasi-lumped components : $\lambda_g/4 < p < \lambda_g/2$ (3.24)

Distributed components : $p > \lambda_g/2$ (3.25)

The MTM being an artificial structure, the average cell size p should be very much less than a quarter wave length i.e., $p << \lambda_g$. Hence as 'rule of thumb effectiveness' condition, the average cell size is set to be $p < \lambda_g/4$. This is also called effective homogeneity limit or condition. It is very difficult to make the structure to be electromagnetically uniform. Effective homogeneity condition ensures the domination of refractive index phenomena over scattering or diffraction phenomena during wave propagation inside MTM medium. If the condition of effective homogeneity is satisfied then, the structure behaves like a real material. That is, the EM waves are essentially myopic to the lattice and the consecutive parameters ε

and μ depend on the nature of the unit cell. Now, the structure is electromagnetically uniform along the direction of propagation.

3.4.3 Preparation of MTM

MTM is an artificial medium tailored for specific EM properties by periodically altering composition of a host dielectric. They are also known as artificial materials having negative ε_r and negative μ_r thereby making the refractive index (n) negative. In conventional materials the refractive index is positive as defined by the ratio of velocity of light in a vacuum to that in medium. Hence, the light travels slower through any given material, or medium, than in vacuum. This is not true in MTM medium where the negative refractive index occurs when the real parts of both ε_{eff} and μ_{eff} have simultaneous negative values as found in Equations (3.26) and (3.27). In the material structures prepared in this way the negative refractive index (NRI) exists over some frequency range only.

$$n = \pm\sqrt{\mu_{eff}\varepsilon_{eff}} \tag{3.26}$$

$$\sqrt{\mu_{eff}\varepsilon_{eff}} = ((e^{-j\pi})(e^{-j\pi}))^{\frac{1}{2}} = \left(e^{-j\frac{\pi}{2}}\right)\left(e^{-j\frac{\pi}{2}}\right) = e^{-j\pi} = -1 \tag{3.27}$$

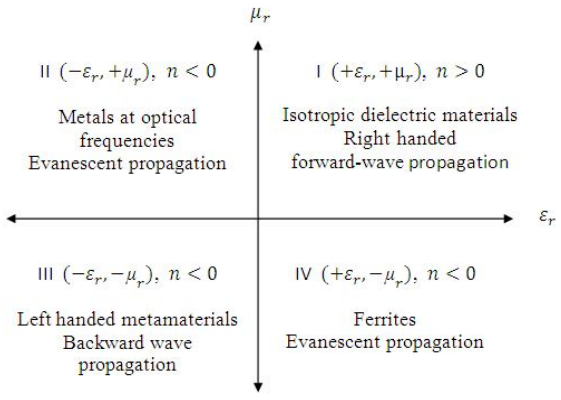

Figure 3.6 Effective Permittivity-Permeability

The negative μ_r and ε_r occur in nature, but not simultaneously. For example silver, gold, and aluminum exhibit negative ε_r at some optical frequencies and ferromagnetic materials exhibit negative μ_r at some resonance frequencies. There are four possible combinations of the pair (ε_r, μ_r) as illustrated in the Figure 3.6 representing the various material media properties. The (ε_r, μ_r), $(-\varepsilon_r, \mu_r)$, $(\varepsilon_r, -\mu_r)$ are the properties of the conventional materials whereas the $(-\varepsilon_r, -\mu_r)$ corresponds to simultaneously negative permittivity and permeability corresponding to the MTMs. The structures exhibiting the simultaneously negative medium properties can be creatively generated on the conventional substrates (Mailadil Sebastian 2008) used for fabrication of antennas.

3.4.4 MTM Structures

There are varieties of structures (Ricardo Marques et al 2007) produced by various researchers on MTM concepts. Starting from simple transmission line (David Smith and Norman Kroll 2000), there exists planar mushroom structure (Christophe Caloz et al 2005), SRRs (circular, elliptical, square, rectangular), CSRRs (complementary of SRRs), S, P, Ω shaped MTM structures (Tie Jun Cui et al 2010) etc. In this work, the square MSRR structure as a MTM and CSRR structure as a defected ground plane are used along with the newly proposed antennas. In microstrip technology there is only one possibility arising. That is, the metallic rings (lines or strips) should be etched as close as possible in order to obtain high magnetic coupling. To enhance coupling either square shaped (Ahmad Sulaiman et al 2010) or rectangular shaped SRRs are preferred. In this way the magnetic flux lines are able to penetrate the strips more efficiently. Each structure has got its own merits.

3.4.5 Resonance in Square Ring MSRR

The formulae for the analytical design of square ring SRR/MSRR, spiral resonators (SR) and labyrinth resonators are well defined (Filiberto

Biloti et al 2007) in literature. The EM behavior of these rings in the quasi-static regime depends on the capacitance and inductance associated with the structures. This is applicable when the inclusions are much smaller than the operating wavelength. Also the mutual interactions between nonadjacent segments and rings are neglected. When the artificial magnetic inclusions (rings) are used to prepare MTM substrates immersed in air, then the resonance can be obtained from the L and C elements in the equivalent LC series circuit as depicted in Figure 3.7.

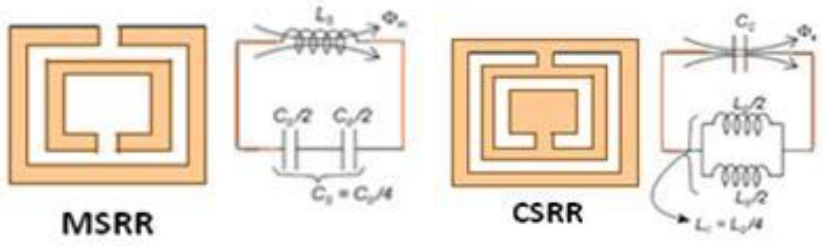

(a) (b)

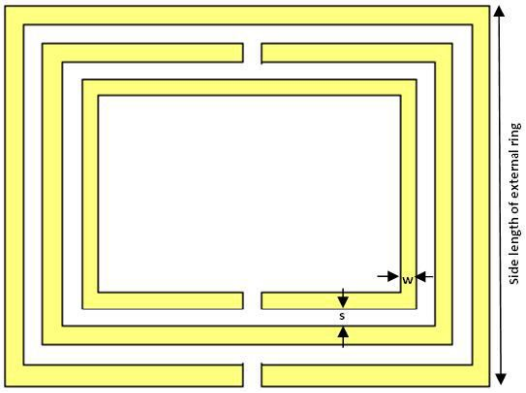

(c)

Figure 3.7 MTM Structures and Their Equivalent Circuits (a) MSRR (b) CSRR (c) Dimensions of MSRR [Courtesy: Filiberto Biloti et al 2007]

The presence of a dielectric substrate with which the MSRR appears, does not affect the inductance. Therefore, its expression is given by Equation (3.28) which is supported by Equations (3.29) - (3.30).

$$L^{MSRR} = \frac{\mu_0}{2}\ \frac{l_{avg}}{4} 4.86\ \left[\ln\left(\frac{0.98}{\rho}\right) + 1.84\,\rho\right] \tag{3.28}$$

where μ_0 is the vacuum permeability

l is the side length of the external ring

ω is the width of the strips and

s is the separation between two adjacent strips

The average strip length l_{avg} calculated over all the N rings is given by

$$l_{avg} = 4[\,l - (N-1)(\omega + s)] \tag{3.29}$$

The filling ratio ρ is given by

$$\rho = (N-1)(\omega + s)/[\ l - (N-1)\ (\omega + s)] \tag{3.30}$$

Now the expression of the capacitance is also given by the Equation (3.31).

$$C^{MSRR} = \frac{N-1}{2}[2\,l - (2N-1)(\omega + s)]C_0 \tag{3.31}$$

The per-unit-length capacitance C_0 between two parallel strips having width ω and separation s is the presence of a dielectric substrate of height h and relative permittivity ε_r are given by Equation (3.32) which is supported by Equations (3.33) and (3.34).

$$C_0 = \varepsilon_0 \varepsilon_{eff}(\varepsilon_r, h, \omega, s)\frac{K(\sqrt{(1-k^2)})}{K(k)} \quad (3.32)$$

where ε_0 is the vacuum permittivity,

$$K(k) = \frac{\pi}{4} + \frac{\pi}{8}\frac{k^2}{1-k^2} - \frac{\pi}{8}\frac{k^4}{1-k^2} \quad (3.33)$$

where K is the complete elliptic integral of the first kind.

The parameter k is given by $k = \frac{s}{s+2\omega};\ 0 \le k \le 1$ (3.34)

and the effective relative permittivity ε_{eff} of the substrate is given by

$$\varepsilon_{eff}(\varepsilon_r, h, \omega, s) = 1 + \frac{2}{\pi} arctg\left[\frac{h}{2\pi(\omega+s)}\right](\varepsilon_r - 1) \quad (3.35)$$

Finally the resonance of the structure is given by the Equation (3.36).

$$f_0 = \frac{1}{2\pi\sqrt{L^{MSRR}C^{MSRR}}}\ \text{GHz} \quad (3.36)$$

The MATLAB coding for resonance calculation of square MSRR is listed in Appendix 3.

3.4.6 MTM Loaded Antenna

The proposed antenna can be loaded on the MTM substrate and verified as described in the previous sections. This loading is nothing but placing some materials on or around an antenna element which may be classified (Kazuhiro Hirasawa and Misao Haneishi 1992) into three categories such as

- Loading with resistive or reactive elements (L and C)
- Loading with dielectric or magnetic materials

- Loading with conducting materials

Radiation may occur from the loaded material along with antenna and one or more than one of these techniques may be used simultaneously. Shaped beam and improved gain of antennas are possible with the presence of MTM structures by controlling the width, spacing, length or by changing the number of such strips involved in the structure.

3.4.7 Simulation Set up for Parameter Retrieval of MTM

Elements providing negative permittivity and negative permeability should be placed in such a way that the interaction between its elements through its quasi-static fields is minimized. However for determining the properties of the MTM medium, HFSS is preferred as it has boundary settings feature which is not found in IE3D. The Figure 3.8 represents the simulation set up in HFSS work space. After creating the MTM structure it should be placed in a suitable boundary environment. The PE (perfect electric) boundary on two sides of x-axis, PM (perfect magnetic) boundary on two sides of z-axis and the waveports 1 and 2 on both sides of y-axis should be set up and then simulated with appropriate solution and sweep frequency ranges. The S parameters thus obtained will have S_{11}, S_{21}, S_{12} and S_{22} since there are two ports. These are complex numbers having real and imaginary parts. The negative medium properties can then be determined by making use of any one of the appropriate methods described briefly in Section 3.4.8.

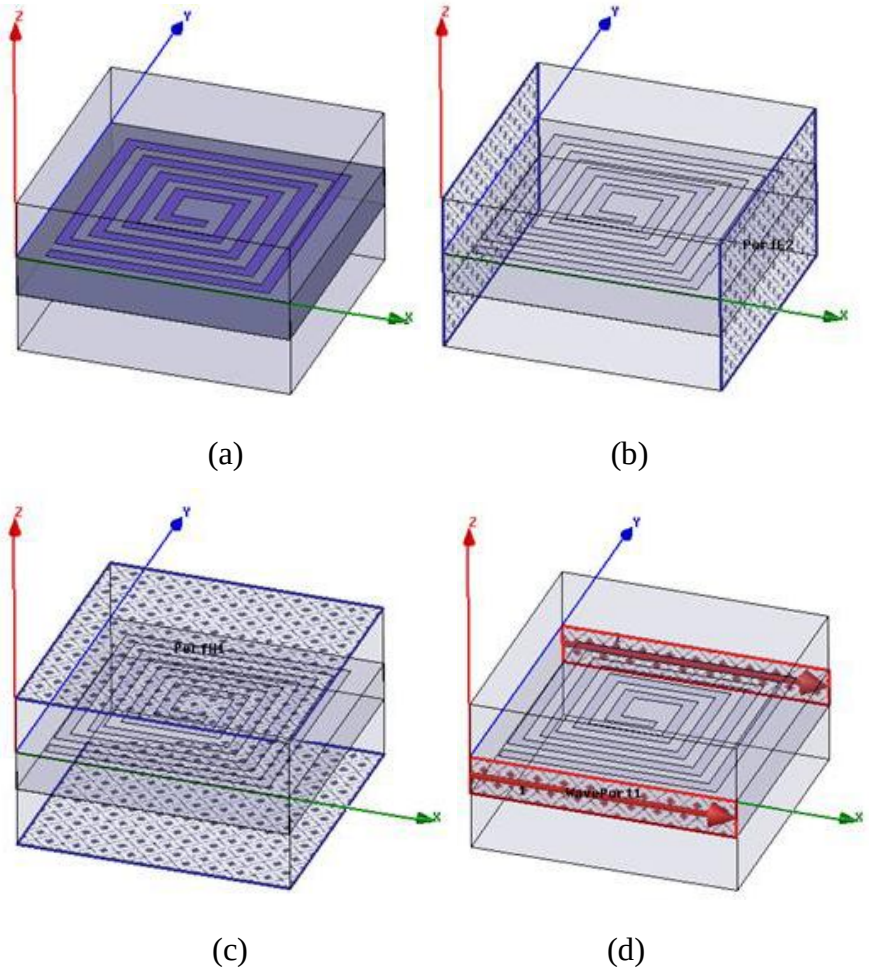

(a) (b)

(c) (d)

Figure 3.8 HFSS Simulation Set up for MTM S Parameters Retrieval (a) Sample MTM Structure (b) PE Boundary (c) PM Boundary (d) Waveports 1 and 2

Using the S parameters data obtained from the simulation, in the Equations from (3.37) to (3.41) for verification of negative medium, the properties ε_r, μ_r and refractive index n can be obtained and also drawn as a function of frequency.

3.4.8 Verification of MTM properties

The Table 3.1 depicts the various methods described by Rohde and Schwarz (2006) for the verification of negative medium properties. The four

popular methods are Nicolson-Ross-Wier (NRW), NIST iteration technique, new non-iterative technique (NNIT) and short circuit techniques (SCT). The selection of the retrieval technique is based on some constraints such as the measured S- parameters, length of the substrate, the required dielectric properties, time involved in the conversion process and the accuracy of the obtained results. The SCT is suitable for one port measurement and hence has the possibility of determining relative permittivity only. The NRW is straight forward, fast, non-iterative and simple. It takes care of effect of magnetic materials also. In NRW itself there are four measurement techniques such as transmission/ reflection line, open ended coaxial probe, free space and resonant type, with regard to the type of substrate material used. The permittivity and permeability of the medium are related to S-parameters by the Equations (3.27) - (3.28).

$$\varepsilon_r = \frac{2}{jkod}\frac{1-V1}{1+V1} \tag{3.37}$$

$$\mu_r = \frac{2}{jk_0 d}\frac{1-V_1}{1+V_1} \tag{3.38}$$

where $$V_1 = S_{21} + S_{11} \tag{3.39}$$

$$V_2 = S_{21} - S_{11} \tag{3.40}$$

and $$n = \sqrt{\varepsilon_r \mu_r} \tag{3.41}$$

where k_0 is a wave number equivalent to $2\pi/\lambda_0$, d is the thickness of the substrate and V_1 and V_2 are terms representing the composite of S_{11} and S_{21} as given in Equations (3.29) and (3.30). The term $k_0 d$ is expected to be very much less than unity for meeting the condition that the antenna must be smaller in size (David Smith et al 2005, Shyam Pattnaik et al 2010). The

corresponding MATLAB coding for verification of negative medium properties is listed for NRW method in Appendix 4.

Table 3.1 Comparison of Different S Parameter Retrieval Techniques [Courtesy: Rohde and Schwarz 2006]

S.No	Algorithm, Measured parameters and possible medium properties	Material type And number of ports	Merits	Limitations
1	NRW $S_{11}, S_{21}, S_{12}, S_{22}$ or S_{11}, S_{21} ε_r and $\mu_r = 1$	Magnetic materials; two port	Fast, non-iterative	Divergent, need for short sample, not suitable for low loss materials
2	NIST $S_{11}, S_{21}, S_{12}, S_{22}$ or S_{11}, S_{21} ε_r and $\mu_r = 1$	Non-magnetic materials; two port	Smooth ε_r, accurate, arbitrary length of sample, no divergence, accommodates low and high loss materials	Measures ε_r only, initial guess for permittivity needed
3	NNIT $S_{11}, S_{21}, S_{12}, S_{22}$ or S_{11}, S_{21} ε_r and $\mu_r = 1$	Magnetic materials; two port	Fast, non-iterative, smooth ε_r, accurate, arbitrary length of sample, no divergence, accommodates low and high loss materials, no initial guess needed	Measures ε_r only
4	SCT S_{11} ε_r only	One port measurement	Smooth ε_r, no divergence, arbitrary length of sample	Measures ε_r only, initial guess needed, iterative, need for accurate sample length

3.5 DESIGN ASPECTS OF IA

Unlike the past where the medical data being recorded in the corporate information management systems, they can be made directly available to physicians through IMDs. Prior to the establishment of MICS (Medical Implant Communications Service), the medical implant devices had to be magnetically coupled to the external devices (Kamya Yekeh Yazdandoost and Ryuji Kohno 2007). Due to this the patient had to be in very close proximity to the external monitoring device often requiring body contact for proper operation. Moreover, medical implant devices were operated with a very slow data rates due to inductive communication and consumed more time for data transfer. With the invention of devices working with wireless coupling, a drastic change is experienced. The MSA configurations are found extensively advantageous for potential use in communication with medical implant devices. When they are laid in IMDs with suitable bio-compatible substrates they are termed as IAs.

3.5.1 Need for Multiband and/or Broadband Functionality

Normally a single antenna has been in use traditionally for wireless link between air and human system. This link should also be robust enough to withstand the patient's movement. Hence, achieving efficient communication in large bandwidth with effective coupling is very challenging with single frequency link. Based on the resonant characteristics of the antenna inside a human body, an implanted antenna can be designed for biomedical applications. Maximum available power is calculated to estimate the required sensitivity of an outside receiver for the wireless link. Therefore recent (Yasir Ahmed et al 2008) needs indicate that multi-functionality implantable antennas are most preferred for operating in multiple frequency bands.

3.5.2 Power Source for IMDs

There are two major categories of IMDS. These devices are either battery-less and should be continuously powered from an external portable battery or have miniature rechargeable batteries that should be inductively charged regularly. There are various button type batteries (Azad and Ali 2006) used as power sources. Once implanted, they are required to be in operation continuously for about 15 to 20 years depending on the application. The shape of implant case containing whole communication circuitry will determine the type of antenna to be used. A flat antenna could be appropriate for pacemaker device while a helical antenna is preferred for urinary implant application. For endoscopy, the smart pills with circular patch antennas are preferred. The antenna size is decided based on the dimensions of the power source also. The antenna in such case is placed on the surface of the battery which is acting as a finite ground plane.

3.5.3 Certain Important Considerations on the Design of IAs

There are certain constraints reported by various implantable antenna investigators which may be considered while designing IAs.

- Size and shape of the antenna (Kamya Yekeh Yazdandoost and Ryuji Kohno 2007, Pichitpong Soontornpipit et al 2004, Xueyi Yu et al 2008).
- Selection of biocompatible material, more losses if the substrate thickness reduces, high quality factor discourages impedance bandwidth, substrate of larger permittivity reduces impedance bandwidth and the location of feed for providing the impedance matching point (Pichitpong Soontornpipit et al 2004).

- Use of superstrate to protect human tissue and acceptable limits for Specific Absorption Rate (SAR, 1.6W/kg) (Yahya Rahmat-Samii 2007).

- Reduction in radiation efficiency due to power absorption in human body (Suresh Atluri and Maysam Ghovanloo 2005, Gupta 2010).

- Gain and impedance bandwidth depends on patch volume - so introduction of slits, slots or irises has a negative effect, the use of edge-shorted patch for miniaturization reduces the physical length by half because shorting component acts as a quarter wave structure (Xueyi Yu et al 2008).

- The shorting pin loading disturbs the field distribution and therefore the resonance happens for various modes (Azad and Ali 2006, Xueyi Yu et al 2008).

- Need for shifting to higher frequency for large and fast data transfer (Yasir Ahmed et al 2008)

3.6 MICROSTRIP LOW PASS FILTER

From the equivalent circuit model found in literatures (Jia-Shen Hong and Lancaster 2001, Collin 2001, David Pozar 2005) the conventional microstrip low pass filter can be designed. This section provides the design aspects of Chebyshev type low pass filter for both Pi and T sections as depicted in Figure 3.9. The simplified design steps (Annapurna Das and Sisir Das 2007) involved in this filter synthesis are described in Equations (3.42) - (3.65).

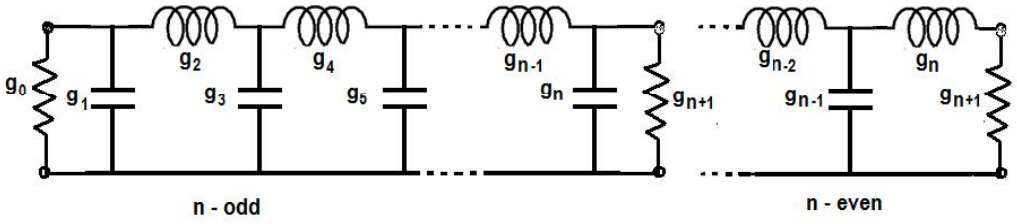

(a)

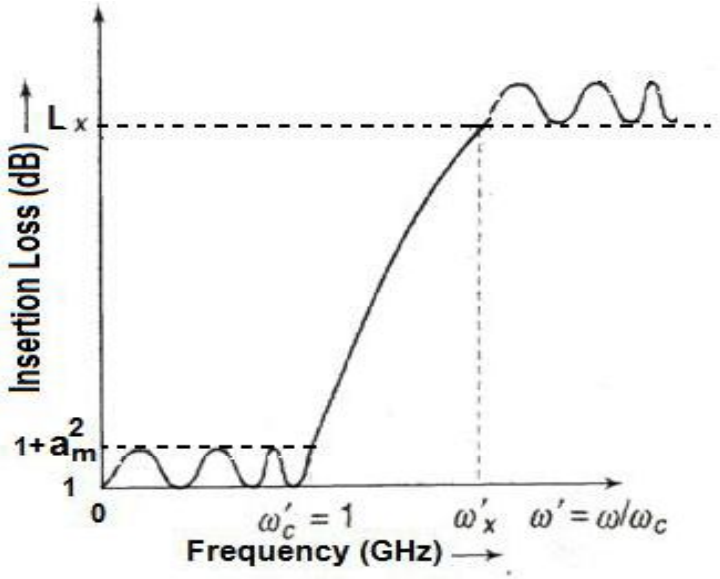

(b)

Figure 3.9 Microstrip Chebyshev Low Pass Filter Section (a) Prototype (b) Insertion Loss (IL) Response
(Source: Annapurna Das and Sisir Das 2007)

$$Ripple\ \ r = 1 + a_m^2 T_n^2(\omega') \tag{3.42}$$

where for stop band attenuation

$$T_n^2(\omega') = 1 \tag{3.43}$$

and for stop band attenuation r_{pba} at f_s,

$$T_n^2(\omega') = \cosh^2(n \cosh^{-1} \omega'_s) \tag{3.44}$$

$$\omega'_s = \omega_s / \omega_c \tag{3.45}$$

where r = ripple (dB)

$T_n(\omega')$=Chebyshev polynomial of degree n

ω_s = angular stopband frequency (GHz)

ω'_s= angular stop band frequency for maximum IL (dB)

ω_c = angular cut-off frequency (GHz)

n = number of elements (excluding source and load impedances)

L_x = represents an insertion loss at a given frequency

$$\frac{W}{h} = \frac{8\,e^A}{e^{2A}-2} \tag{3.46}$$

where $$A = \frac{Z_o}{6}\left[\frac{\varepsilon_r+1}{2}\right]^{1/2} + \frac{\varepsilon_r-1}{\varepsilon_r+1}\left[0.23 + \frac{0.11}{\varepsilon_r}\right] \tag{3.47}$$

W = width of the substrate

h = thickness of the substrate

The characteristic impedance Z_0 is essentially considered to be 50 ohms for matched conditions and ε_r is the relative permittivity of the substrate material. Depending on whether $W/h < 1$ or $W/h \geq 1$, one can choose the appropriate formula for the determination of the effective medium property.

If $W/h < 1$, then the following Equations (3.48) and (3.49) may be chosen

$$\varepsilon_{eff} = \left[\frac{\varepsilon_r+1}{2}\right] + \left[\frac{\varepsilon_r-1}{2}\right]\left[\left(1+\frac{12h}{W}\right)^{-\frac{1}{2}} + 0.04\left(1-\frac{W}{h}\right)\right]^2 \tag{3.48}$$

$$Z_o = \frac{60}{\sqrt{\varepsilon_{eff}}} \ln\left[\left(\frac{8h}{W}\right) + 0.25\left(\frac{W}{h}\right)\right] \quad (3.49)$$

If $W/h \geq 1$, then the following Equations (3.50) and (3.51) may be used.

$$\varepsilon_{eff} = \left[\frac{\varepsilon_r+1}{2}\right] + \left[\frac{\varepsilon_r-1}{2}\right]\left[1 + \frac{12h}{W}\right]^{-1/2} \quad (3.50)$$

$$Z_o = \left[\frac{377}{\sqrt{\varepsilon_{eff}}}\right]\left[\frac{W}{h} + 1.393 + \left(\frac{2}{3}\right)\ln\left(\frac{W}{h} + 1.444\right)\right]^{-1} \quad (3.51)$$

For the inductor, $Z_0 = Z_{0L} = 100$ ohms and for the capacitor $Z_0 = Z_{0C} = 20$ ohms may be used with reference to the Wheeler's curve found in literature (Jia-Shen Hong and Lancaster 2001). The strip width may assume the notations $W_{Tx}, W_{OL}\ and\ W_{OC}$ corresponding to transmission line, inductor and capacitor respectively. The transmission line length can be taken to be multiples of $\frac{\lambda_{go}}{4}$. Moreover for pass band ripple of $0.5\ dB$, the g values are $g_o = 1.0000,\ g_1 = 1.5963,\ g_2 = 1.0969,\ g_3 = 1.5963\ and\ g_4 = 1.0000$. For any other ripple value or for any change in the order of the filter, the appropriate g values can be obtained from the table found in literatures (Annapurna Das and Sisir Das 2007).

The free space wave length $\lambda_o = c/f_c$ (3.52)

where $c = 3\text{x}10\text{^}11\text{mm/sec}$

The wave length through transmission line $\lambda_{go} = \frac{\lambda_o}{\sqrt{\varepsilon_{effTx}}}$ (3.53)

The transmission line (strip) length

$$L_{Tx} = \lambda_{go}/8 \quad (3.54)$$

The wavelength through the inductor

$$\lambda_{gL} = \lambda_o / \sqrt{\varepsilon_{eff}}_{\mathrm{L}} \tag{3.55}$$

The wavelength through the capacitor

$$\lambda_{gC} = \lambda_o / \sqrt{\varepsilon_{eff}}_{\mathrm{C}} \tag{3.56}$$

The procedure for the calculation of all the above quantities is common for both Pi and T section LPF designs with refrence to Figure 3.9(a). Now the exact dimensions of the filter components can be calculated based on the type of filter.

The roll-off rate corresponding to LPF is given by

$$\xi = \frac{\alpha_{\max} - \alpha_{min}}{f_s - f_c} \tag{3.57}$$

where α_{max} and α_{min} are the attenuation points corresponding to f_s and f_c respectively.

For the design of a third order Pi section filter the Equations (3.58) - (3.61) may be used. The dimensions of the components in the filter can be realized accordingly.

Length of inductor strip

$$\beta L_{L2} = L_2 \frac{Z_o}{Z_{oL}} \quad where\ \beta = 2\pi/\lambda_{gL} \tag{3.58}$$

where $$L_2 = \left(\frac{Z_o}{g_0}\right)\left(\frac{\Omega_c}{2\pi f_c}\right) g_2 \text{and}\ \ \Omega_c = 1 \tag{3.59}$$

Length of capacitor strip

$$\beta L_{C1,C3} = C_{1,3}\, Z_{oL}/\, Z_o \quad where\ \beta = 2\pi/\lambda_{gC} \tag{3.60}$$

where $C_1 = C_3 = \left(\frac{g_0}{Z_o}\right)\left(\frac{\Omega_c}{2\pi f_c}\right) g_1$ and $\Omega_c = 1$ (3.61)

For the design of a third order T section filter the Equations (3.62) - (3.65) may be used. The dimensions of the components in the filter can be realized accordingly.

Length of inductor

$$\beta L_{L1,L3} = L_{1,3}\frac{Z_0}{Z_{0L}}\ where\ \beta = 2\,\pi/\lambda_{gL} \tag{3.62}$$

where

$$L_1 = L_3 = (Z_0/g_0)(\ \Omega_c/2\pi f_c)\ g_1 \tag{3.63}$$

Length of capacitor

$$\beta L_{c2} = C_2\frac{Z_{0L}}{Z_0}\quad where\ \beta = 2\pi/\lambda gc \tag{3.64}$$

where

$$C_2 = (\ g_0/Z_0)(\ \Omega_c/2\pi f_c)\ g_2 \tag{3.65}$$

3.7 CONCLUDING REMARKS

This chapter has provided a useful insight into the design aspects of MSA, FA, MTM, IA and LPF. With the ideas and analytical formulae presented the various microstrip components antennas are designed.